IEEE Access
Multidisciplinary | Rapid Review | Open Access Journal

Received 8 July 2022, accepted 25 July 2022, date of publication 28 July 2022, date of current version 4 August 2022.

Digital Object Identifier 10.1109/ACCESS.2022.3194648

RESEARCH ARTICLE

An Operating Mode Based on Variable DC Voltage and Current for Enlarging P–Q Capability Range of Unidirectional Current H-Bridge Submodule-Based MMC

ZHENGXUAN LI[1], (Graduate Student Member, IEEE), LINLIN WU[2], (Associate Member, IEEE), QIANG SONG[1], (Senior Member, IEEE), XIAOYANG DENG[2], BIAO ZHAO[1], (Senior Member, IEEE), YUNHONG LI[2], AND KAILUN WANG[1]

[1]Department of Electrical Engineering, Tsinghua University, Beijing 100084, China
[2]State Grid Jibei Electric Power Company Ltd., Beijing 100045, China

Corresponding author: Qiang Song (songqiang@tsinghua.edu.cn)

This work was supported in part by State Grid Jibei Electric Power Company Ltd. under Grant 52018K21001P, Research on Key Technologies for Safe Operation Control and Equipment Status Diagnosis of VSC-HVDC Transmission System.

ABSTRACT Modular multilevel converters (MMCs) are widely utilized in dc applications. With the development of MMCs, many applications require the MMCs to have additional functions and characteristics, such as dc fault clearing capability and low submodule capacitance. A unidirectional current H-bridge submodule (UCH-SM) has been proposed, which uses low submodule capacitance and possesses dc fault clearing capability. However, the reactive power capability is limited during low active power because of the inadequate dc bias in arm currents caused by the low dc current. Although retaining a rated dc current even at zero active power has been proposed, it results in increasing the power losses and large capacitance. This study proposes a new operating mode based on variable dc voltage and variable dc current (VVVCM) for point-to-point dc systems. The basic idea is that both the dc voltage and current vary on the basis of active power and a lower limit is set for the dc current to provide adequate dc bias in the arm currents during reactive power exchange. Analysis shows that the UCH-MMC in VVVCM has an enlarged P–Q capability range and still retains low capacitor usage. Simulation results verify the effectiveness of the proposed mode.

INDEX TERMS UCH-MMC, variable dc voltage and current mode, P–Q capability range, compactness.

I. INTRODUCTION

Modular multilevel converter (MMC) is emerging as a predominant technology in dc applications [1]–[4]. The modular design enables MMCs to fit different power and voltage ranges with little harmonic distortion. With the development of MMCs, many applications require the MMCs to have additional functions and characteristics. For instance, the overhead line-based high-voltage direct current (HVDC) requires the MMCs to be able to block the dc fault currents [2], [5]. The offshore applications require the MMCs to have small footprint and high power-density [6], [7]. However, the prevailing half-bridge submodule (HBSM)-based MMCs (HB-MMC) cannot clear the dc faults because of the freewheeling diodes [2]. Due to the arm energy fluctuations, the submodule capacitors in the HB-MMCs are commonly extremely large, occupying more than 50% of the volume [8], [9].

Full-bridge submodule (FBSM) was originally proposed for blocking dc fault currents [2]. The FBSM-based MMC can clear the dc faults by blocking the converter. Recent studies have reported that the FBSM can output an additional

The associate editor coordinating the review of this manuscript and approving it for publication was Tariq Masood.

negative voltage, which can be used to increase the modulation index [10]–[16]. It is revealed that the FB-MMCs can reduce the submodule capacitance by increasing the modulation index using the negative voltage states of FBSMs [10]–[16]. For example, the submodule capacitor can be reduced by 70% at unity power factor if the modulation index is increased to approximately 1.414 [10]–[16]. However, an FBSM utilizes twice the number of semiconductors as that of an HBSM, thus increasing the cost, volume, and power losses [2].

To reduce the use of semiconductors, reference [17] has pointed out that the increase in the modulation index can decrease the fundamental-frequency ac component in the arm current, then the arm current tends to be unidirectional. On this prerequisite, an FBSM can be simplified into a unidirectional current H-bridge submodule (UCH-SM) by eliminating two IGBTs [17], [18]. The UCH-SM-based MMC (UCH-MMC) inherits the dc fault capability of the FB-MMC. The increase in the modulation index also enables the UCH-MMC to have extremely small submodule capacitance [19]. Compared with the FB-MMC, the UCH-MMC saves approximately half of the semiconductors [17]. Therefore, the UCH-MMC is an attractive and impressive solution to the future HVDC technique.

However, the prerequisite for the operation of UCH-MMCs is that the arm current must be unidirectional [17]. This condition requires that the dc current must exist to provide sufficient dc bias in the arm currents. However, when the active power is low, the inadequate dc bias results in that the UCH-MMC cannot output high ac current, and thus does not have sufficient reactive power exchange capability [17]. This condition limits the P–Q capability range and increase the difficulty of supporting the grid during transient states. Especially, the reactive power capability is 0 when the active power is 0. Therefore, the UCH-MMC cannot fit many practical applications.

A constant current mode (CCM) was proposed to enlarge the P–Q capability range [17], [19]. The basic idea of CCM is to retain a rated dc current even when the active power is 0 to provide the dc bias for the unidirectional current, while the dc voltage varies proportionally to the active power flow. However, retaining the rated dc current even at zero active power causes high transmission losses. In addition, the rated dc current at low dc voltages changes and increases the arm energy fluctuations [19], [20], thereby increasing the capacitance requirement.

To enlarge the P–Q capability range while maintaining the low submodule capacitance and low power losses, this study proposes a new operating mode based on variable dc voltage and variable dc current (VVVCM) for point-to-point HVDC systems based on UCH-MMCs. In the proposed operating mode, both the dc voltage and current vary according to the active power. However, a lower limit of dc current is set based on the rated reactive power of the UCH-MMC to provide adequate dc bias for the unidirectional arm currents. Detailed analysis shows that the proposed operating mode enlarges the

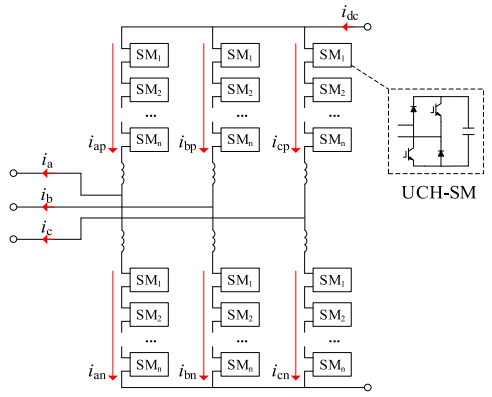

FIGURE 1. Topology of UCH-MMC.

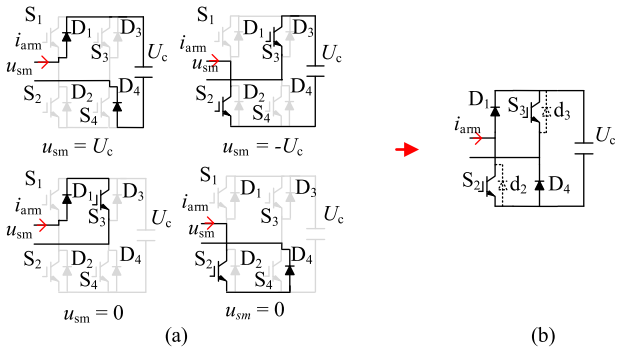

FIGURE 2. Derivation and topology of UCH-SM: (a) Current path in FBSM when current is unidirectional; (b) topology of UCH-SM.

P–Q capability range while retaining low capacitance and low losses. The contributions of this study are listed as follows:

- A VVVCM is proposed for the UCH-MMC;
- Comparison of energy storage requirement is conducted, indicating that the proposed VVVCM makes a trade-off between the P–Q capability range and capacitor usage;
- Power loss analysis result indicate that the VVVCM can extremely reduce the power losses compared with the CCM.

II. EXISTING OPERATING MODES OF UCH-MMC

A. PRINCIPLE OF UCH-MMC

Fig. 1 shows the topology of UCH-MMC [17]. The converter arms are composed of UCH-SMs, which are variants of FBSM. The diodes d_2 and d_3 are only for pre-charging the converter, and thus, are of small capacities. Fig. 2(a) shows the current path when the current is unidirectional, where no current flows through the IGBTs S_1, S_4 and diodes D_2, D_3 [17]. Then an FBSM can be simplified into a UCH-SM, as shown in Fig. 2(b), which by comparison utilizes half the IGBTs but can still output positive, zero, and negative voltage levels.

Based on Fig. 1, if the natural circulating currents are neglected, the arm currents can be written as:

$$\begin{cases} i_{xp} = \dfrac{1}{3} i_{dc} + \dfrac{1}{2} i_x \\ i_{xn} = \dfrac{1}{3} i_{dc} - \dfrac{1}{2} i_x, \end{cases} \tag{1}$$

where x = a, b, c; i_{xp} and i_{xn} are the upper and lower arm currents of phase x; i_x denotes the phase currents; and i_{dc} is the dc current. The phase currents i_a, i_b, and i_c are:

$$\begin{cases} i_a = \sqrt{2}\, I_{ac} \cos(\omega t - \varphi) \\ i_b = \sqrt{2} I_{ac} \cos(\omega t - \varphi - 2\pi/3) \\ i_c = \sqrt{2} I_{ac} \cos(\omega t - \varphi + 2\pi/3), \end{cases} \tag{2}$$

where I_{ac} is the RMS value of the ac currents and φ is the power factor angle.

The condition for the operation of UCH-MMC is that the arm current must be unidirectional, that is, i_{xp}, $i_{xn} \geq 0$. Therefore, the following relationship must be met to maintain unidirectional arm currents:

$$I_{ac} \leq \frac{\sqrt{2}(1-3h)}{3} i_{dc}, \tag{3}$$

where h represents the harmonic distortion in the dc current [17]. In an HVDC application, the harmonic current of MMCs is usually small, and an h value of 1% is usually sufficiently high [17].

The power relationship between the ac and dc sides of an MMC is:

$$U_{dcN} i_{dc} = 3 U_{acN} I_{ac} \cos\varphi, \tag{4}$$

where U_{dcN} and U_{acN} are the rated dc and ac voltages. Substituting (4) into (3), the ac voltage should meet:

$$U_{acN} \geq \frac{\sqrt{2}}{2(1-3h)\cos\varphi_{max}} \times U_{dcN}, \tag{5}$$

where φ_{max} is the maximum power factor angle.

However, the ac voltage requirement in (5) exceeds twice that of the conventional HB-MMC, which may induce difficulties for insulation designs. To alleviate this problem, an active circulating current was proposed as follows [17]:

$$\begin{cases} i_{cira} = \left|\frac{i_a}{3}\right| - \left|\frac{i_b}{6}\right| - \left|\frac{i_c}{6}\right| \\ i_{cirb} = \left|\frac{i_b}{3}\right| - \left|\frac{i_c}{6}\right| - \left|\frac{i_a}{6}\right| \\ i_{circ} = \left|\frac{i_c}{3}\right| - \left|\frac{i_a}{6}\right| - \left|\frac{i_b}{6}\right|. \end{cases} \tag{6}$$

The arm current after injecting the active circulating current then becomes:

$$\begin{cases} i_{xp} = \frac{1}{3} i_{dc} + \frac{1}{2} i_x + i_{cirx} \\ i_{xn} = \frac{1}{3} i_{dc} - \frac{1}{2} i_x + i_{cirx}. \end{cases} \tag{7}$$

By injecting the active circulating currents, voltage and current requirements are reduced [17]:

$$U_{acN} \geq \frac{\sqrt{2}}{3(1-3h)\cos\varphi_{max}} \times U_{dcN}, \tag{8}$$

$$I_{ac} \leq \frac{\sqrt{2}(1-3h)}{2} i_{dc}. \tag{9}$$

The conditions in (8) and (9) are more feasible than those in (3) and (5), and are thus used as basis for the following analyses.

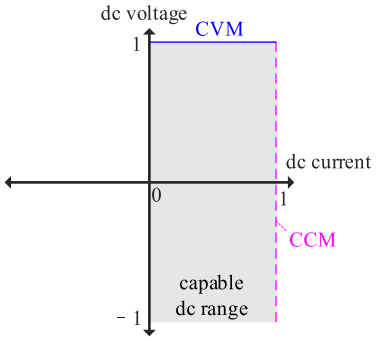

FIGURE 3. Capable dc range and operating ranges of CVM and CCM.

B. CAPABLE DC RANGE AND OPERATING RANGES OF CONSTANT VOLTAGE AND CONSTANT CURRENT MODES OF UCH-MMC

The UCH-SM and UCH-MMC only allow unidirectional currents. However, given that the UCH-SM can output a negative voltage level, the UCH-MMC has a wide dc voltage range from negative to positive rated values. Fig. 3 shows the dc range of the UCH-MMC as the shaded area.

On the one hand, the UCH-MMC can operate in constant voltage mode (CVM) [17], as shown by the solid line in Fig. 3. Similar to the conventional HB-MMC, the dc voltage is at the rated value while the dc current varies to fit the active power flow. In CVM, the dc and ac currents can be expressed by:

$$\begin{cases} i_{dc} = \dfrac{P}{U_{dcN}} \\ I_{ac} = \dfrac{\sqrt{P^2+Q^2}}{3U_{acN}}, \end{cases} \tag{10}$$

where P and Q are the active and reactive powers, respectively.

Substituting (10) into (9) yields:

$$|Q| \leq \sqrt{\frac{9}{16}m^2 - 1} \times |P| \times (1-3h), \tag{11}$$

where m is the modulation index defined as:

$$m = \frac{\sqrt{2}U_{acN}}{U_{dcN}/2}. \tag{12}$$

The rated active power is denoted by P_N, and thus $P_N = U_{dcN} I_{dcN}$. Normalizing (11) by P_N yields:

$$|Q_{pu}| \leq \sqrt{\frac{9}{16}m^2 - 1} \times |P_{pu}| \times (1-3h). \tag{13}$$

According to (13), Fig. 4 shows that the reactive power of the UCH-MMC in CVM is limited by the active power because the dc bias in the arm current is provided by the dc current. Especially when the active power is zero, the UCH-MMC has no reactive power capability. However, an MMC is required to exchange reactive power with the power grid even when the active power is zero. This disadvantage of the UCH-MMC in CVM restricts its application to a great extent.

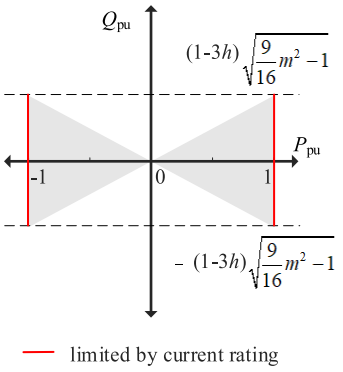

FIGURE 4. P–Q capability range of UCH-MMC in CVM.

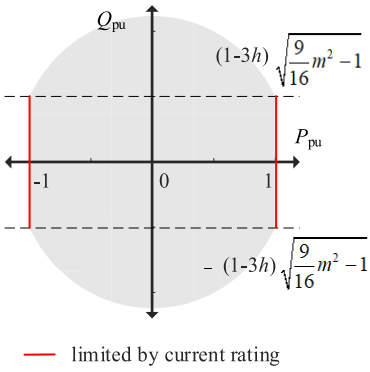

FIGURE 5. P–Q capability range of UCH-MMC in CCM.

A constant current mode (CCM) was proposed to enlarge the P–Q capability range of UCH-MMC [17], [19]. The basic idea is that the dc current retains its rated value even at zero active power, while the dc voltage varies proportionally to the active power, as shown by the dashed line in Fig. 3. The advantage of CCM is that the dc current can provide adequate dc bias in the arm current for reactive power generation. In CCM, the dc and ac currents can be expressed by:

$$\begin{cases} i_{dc} = I_{dcN} \\ I_{ac} = \dfrac{\sqrt{P^2+Q^2}}{3U_{acN}}. \end{cases} \tag{14}$$

Substituting (14) into (9) yields:

$$P^2 + Q^2 \le \frac{9}{16} m^2 P_N^2 \times (1-3h)^2 . \tag{15}$$

Normalizing (15) with P_N yields:

$$P_{pu}^2 + Q_{pu}^2 \le \frac{9}{16} m^2 \times (1-3h)^2 . \tag{16}$$

Fig. 5 shows the P–Q capability range of UCH-MMC in CCM. The reactive power is no longer limited by the active power in CCM. However, retaining the rated dc current results in large power losses in both the converters and transmission lines. In addition, the rated dc current at low dc voltages also generates high energy fluctuations on the submodule capacitors [19], [20], restricting the reduction effects on capacitance.

III. PROPOSED OPERATING MODE OF UCH-MMC BASED ON VARIABLE DC VOLTAGE AND VARIABLE DC CURRENT

A. PRINCIPLE OF THE PROPOSED MODE

As discussed in Section II, both the existing CVM and CCM of UCH-MMC have evident disadvantages. Therefore, this study proposes a new operating mode based on variable dc voltage and variable dc current (VVVCM). The basic idea of the VVVCM is that both the dc voltage and current vary according to the active power, but a lower limit is set based on the rated reactive power of the UCH-MMC to provide adequate dc bias for the unidirectional arm currents. By implementing the VVVCM, the UCH-MMC can attain adequate P–Q capability range, maintain low losses, and demand small submodule capacitors.

The ac current of UCH-MMC can be written in a power–voltage form as:

$$I_{ac} = \frac{\sqrt{P^2+Q^2}}{3U_{acN}}. \tag{17}$$

Substituting (17) into (9), the dc current requirement is:

$$i_{dc} \ge \sqrt{2} \times \frac{\sqrt{P^2+Q^2}}{3U_{acN} \times (1-3h)}. \tag{18}$$

Thus, expression (18) is the minimum dc current requirement of a UCH-MMC at a given active and reactive power. However, the requirement in (18) cannot be applied to a UCH-MMC-based HVDC system because the sending- and receiving-end MMCs may have different reactive powers. Given that the MMC usually transmits active power, the reactive power capability is commonly limited to lower than 0.5 p.u. In several offshore applications, the reactive power is even limited to 0.2–0.3 p.u. to facilitate the design. Therefore, the reactive power Q in (18) can be replaced by its rated value Q_N, and then the dc current reference is:

$$i_{dc}^* = \sqrt{2} \times \frac{\sqrt{P^2+Q_N^2}}{3U_{acN} \times (1-3h)}. \tag{19}$$

As such, the only variable on the right hand of (19) is the active power. That is, the dc current reference varies only according to the active power. Fig. 6 shows the dc operating range of UCH-MMC in VVVCM as the dash-dotted line. The dc current decreases when the active power decreases, but never reaches zero to provide the dc bias in the arm currents.

Based on (19), the dc voltage reference can be calculated as:

$$u_{dc}^* = \frac{P}{i_{dc}^*} = \frac{3U_{acN} \times (1-3h) \times P}{\sqrt{2} \times \sqrt{P^2+Q_N^2}}. \tag{20}$$

Assuming that the system is in steady state, the dc current follows its reference, that is, $i_{dc} = i_{dc}^*$. Then, substituting (17) and (19) into (9), the P–Q capability range is:

$$|Q| \le |Q_N| . \tag{21}$$

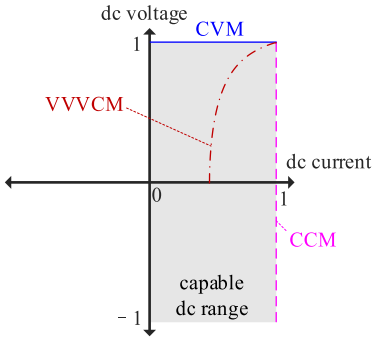

FIGURE 6. Capable dc range and operating ranges of CVM, CCM and VVVCM.

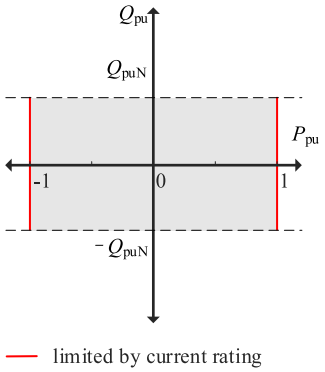

FIGURE 7. P–Q capability range of UCH-MMC in VVVCM.

Normalizing (21) by the rated active power P_N, then the P–Q capability range can be expressed by the per-unit values as:

$$\left|Q_{pu}\right| \leq \left|Q_{puN}\right|. \tag{22}$$

Fig. 7 shows the P–Q capability range of the UCH-MMC in VVVCM. Using the proposed VVVCM, the reactive power is no longer limited by the active power, and its range can be designed by designing the parameter Q_N.

B. ECONOMIC COMPARISON

The total capacitor usage in an MMC is affected by the submodule capacitance, rated voltage of each capacitor, and the total number of submodules [21], [22]. Therefore, an energy storage requirement is defined below to indicate the total usage of capacitors [22]:

$$E_{MMC} = 6 \times \frac{1}{2} C_{SM} U_{CN}^2 \times N, \tag{23}$$

where C_{SM} is the submodule capacitance, U_{CN} is the rated voltage of the capacitor, and N is the number of submodules per arm.

The interaction between the arm current and voltage generates the power fluctuation in the converter arm. In addition, the energy fluctuation is the integral of the power fluctuation, which can be expressed using:

$$e_{arm} = \int p_{arm}\, dt = \int u_{arm} i_{arm}\, dt, \tag{24}$$

TABLE 1. Basic parameters of the UCH-MMC example.

Terms	Values
Rated active power / MW	1000
Rated reactive power (Q_N) / Mvar	500
Rated dc voltage / kV	640
Rated ac voltage / kV	348

where e_{arm} and p_{arm} are the energy and power fluctuations in the converter arm, respectively; and u_{arm} and i_{arm} are the arm voltage and current, respectively. Given that the MMC operates symmetrically, the lower arm of phase A is taken as an example. Based on (7), the arm current is:

$$i_{an} = \frac{1}{3} i_{dc} - \frac{1}{2} i_a + i_{cira}, \tag{25}$$

where i_a and i_{cira} are expressed in (2) and (6) in the previous section. The arm voltage is:

$$u_{an} = \frac{1}{2} u_{dc} + u_a - u_{Lan}, \tag{26}$$

where u_{dc} is the dc voltage, u_a is the grid voltage of phase A, and u_{Lan} is the voltage that drops on the arm inductor. The expressions of u_a and u_{Lan} are:

$$u_a = \sqrt{2} U_{acN} \cos \omega t, \tag{27}$$

$$u_{Lan} = L_{arm} \frac{di_{an}}{dt}, \tag{28}$$

where L_{arm} is the arm inductance. The expression of u_{Lan} is difficult to obtain because various harmonics exist in the arm current. However, the value of u_{Lan} varying with time can be calculated using numerical programs based on (28).

The upper limit of the voltage ripple rate of the submodule capacitor is denoted by ε_{lim}. Assuming that the energy fluctuation in (24) is evenly distributed in each submodule, then the following relationship must be met:

$$\frac{1}{2} C_{SM} U_{CN}^2 + \frac{e_{arm}}{N} \leq \frac{1}{2} C_{SM} \left(1 + \varepsilon_{lim}\right)^2 U_{CN}^2. \tag{29}$$

From (29), the energy storage requirement must meet:

$$E_{MMC} \geq \frac{6 \times e_{arm}}{\left(1 + \varepsilon_{lim}\right)^2 - 1}. \tag{30}$$

The value of e_{arm} not only varies with time, but also based on the operating points of the UCH-MMC, that is, P and Q. Therefore, to ensure the establishment of (30), the energy storage requirement must be greater than the maximum value of e_{arm}, that is, the maximum amplitude of e_{arm} in the entire operating range. Therefore, the energy storage requirement of an MMC is:

$$E_{MMC} \geq \frac{6E_{arm-max}}{\left(1 + \varepsilon_{lim}\right)^2 - 1}, \tag{31}$$

where $E_{arm-max}$ is the maximum amplitude of e_{arm} in the entire operating range.

A 1000MW/±500Mvar UCH-MMC is taken as a study case. TABLE 1 shows the parameters. The maximum amplitudes of the energy fluctuations in a UCH-MMC arm are

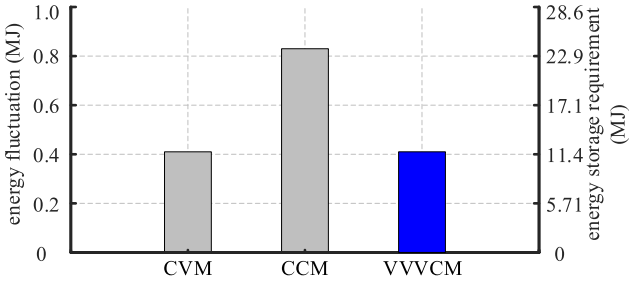

FIGURE 8. Comparison of energy fluctuations and energy storage requirements of UCH-MMCs among CVM, CCM and VVVCM.

TABLE 2. Energy storage requirements under different values of Q_N.

Rated reactive power (Q_N) / Mvar	100	200	300	400	500
Amplitude of energy fluctuation / MJ	0.26	0.28	0.32	0.36	0.41
Energy storage requirement / MJ	7.37	8.06	9.00	10.17	11.62

calculated based on CVM, CCM and VVVCM, respectively. Fig. 8 shows the calculation results. By comparing the existing operating modes, the UCH-MMC in CVM has much lower energy fluctuation and energy storage requirement than that in the CCM. However, as pointed out in the previous section, the UCH-MMC in the CVM cannot fit the practical applications because of the inadequate P–Q capability range. Yet, the UCH-MMC in the CCM requires too high energy storage requirement, resulting in large footprint of the MMC, despite the enhancement of the reactive power capability. The proposed VVVCM can make a trade-off between enhancement of the reactive power capability and the energy storage requirement. On the one hand, the P–Q capability range is enlarged compared with the CVM, enabling the UCH-MMC to fit the practical applications. On the other hand, the VVVCM will not increase the energy storage requirement.

TABLE 2 presents the amplitudes of energy fluctuations and energy storage requirements when the rated reactive powers are 100–500 Mvar. The results show that the VVVCM-based UCH-MMC has low energy storage requirement in a wide range of rated reactive powers.

A power loss comparison is conducted between the CCM and VVVCM. Both the CCM and the VVVCM can enlarge the P–Q capability range, but the VVVCM has much less power losses than the CCM. Therefore, the VVVCM is more economical in operation.

IV. CONTROL STRATEGY OF UCH-MMC IN VVVCM

Fig. 10 shows the control strategy of the UCH-MMC in VVVCM. In a real end-to-end HVDC system, one of the two MMCs controls the dc current while the other controls the dc voltage. Fig. 10 shows the controls strategies for the current- and voltage-control MMC. For the current-control MMC, the dc current reference of the current-control MMC is generated based on (19). For the voltage-control MMC,

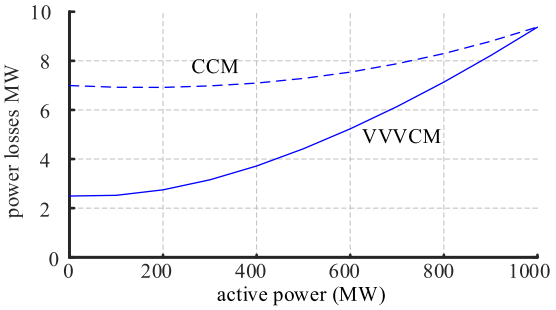

FIGURE 9. Power loss comparison between CCM and VVVCM.

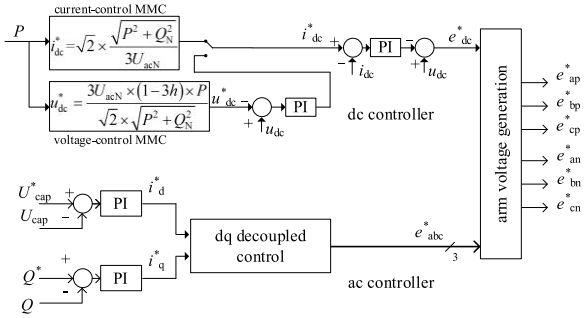

FIGURE 10. Control Strategy of UCH-MMC in VVVCM.

the dc voltage reference is generated based on (20), and a close-loop dc voltage controller is implemented. The output of the dc voltage controller is the dc current reference, and a closed-loop current controller is implemented to make the dc current follow the reference. The output of the dc controller is the dc intermediate control variable (ICV) e^*_{dc}.

The capacitor voltage indicates the power balance between the ac and dc sides. Therefore, an outer-loop PI controller of the capacitor voltage is used to generate the d-axis current reference i^*_d. The q-axis current reference i^*_q is generated by the reactive power controller. The classical d- and q-axis decoupled controller is implemented in the inner loop and generates the three-phase ac ICVs, e^*_a, e^*_b, and e^*_c. Finally, using the dc and ac ICVs, the arm voltage references can be obtained using [23]:

$$\begin{cases} e^*_{xp} = \dfrac{e^*_{dc}}{2} - e^*_x \\ e^*_{xn} = \dfrac{e^*_{dc}}{2} + e^*_x, \end{cases} \tag{32}$$

where x = a, b, c, and e^*_{xp} and e^*_{xn} denote the reference voltages of the upper and lower arms of phase x, respectively.

V. SIMULATION RESULTS

The proposed VVVCM is verified through simulation results. Fig. 11 shows the structure of the studied system. The electrical parameters of the UCH-MMCs in the simulation are the same as those in TABLE 1, and other parameters are listed in TABLE 3. The receiving-end UCH-MMC controls the dc current of the system while the sending-end UCH-MMC controls the dc voltage. A diode is connected to the dc lines to create a current path for the receiving-end UCH-MMC during start-up. The models were built and the simulation were con-

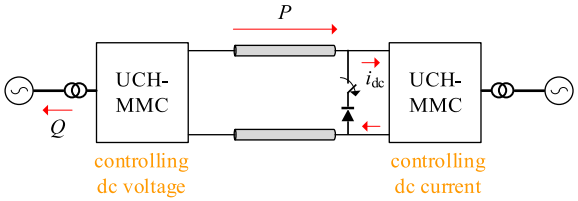

FIGURE 11. Simulation model.

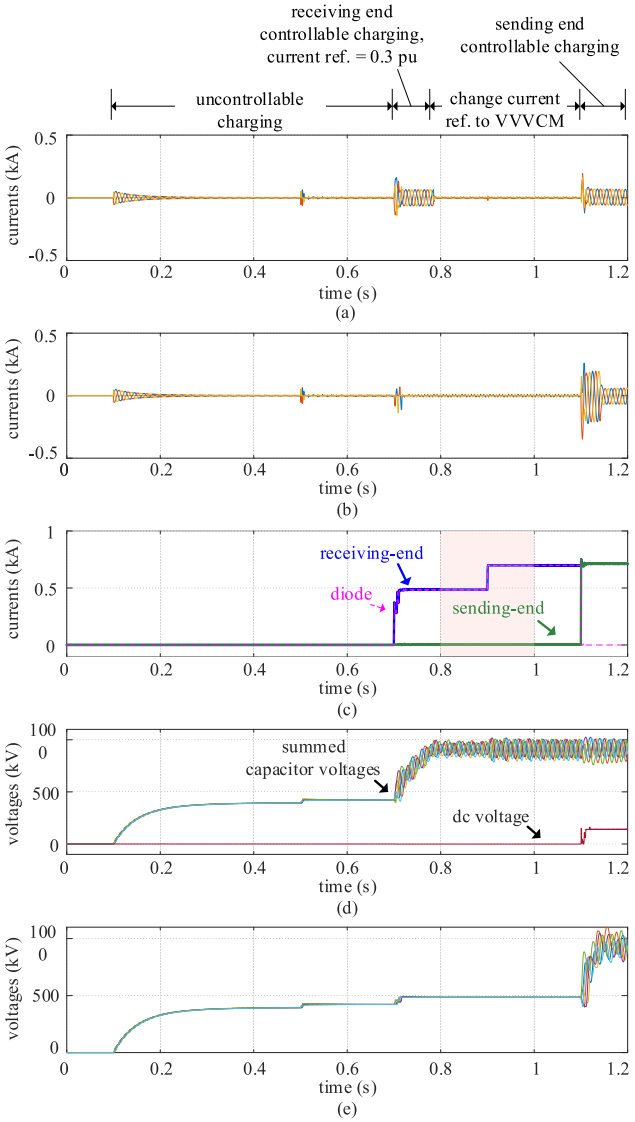

FIGURE 12. Simulation results during start-up state: (a) Receiving-end ac currents; (b) sending-end ac currents; (c) dc currents and diode current; (d) receiving-end summed capacitor voltages and dc voltage; and (e) sending-end summed capacitor voltages.

ducted both in MATLAB/Simulink and PSCAD/EMTDC. The simulation results using these two simulation tools are well consistent. Due to the limited space, only the results obtained in Matlab/Simulink are shown.

A. SIMULATION OF START-UP

Fig. 12 shows the simulation results during the start-up stage, when the circuit breaker connected with the diode is closed. The uncontrollable charging of the MMCs in the simulation

TABLE 3. Parameters of UCH-MMCs in simulation.

Terms	UCH-MMC
Numbers of SMs per arm	562
SM capacitance / mF	2.692
Arm inductance / mH	0.1951

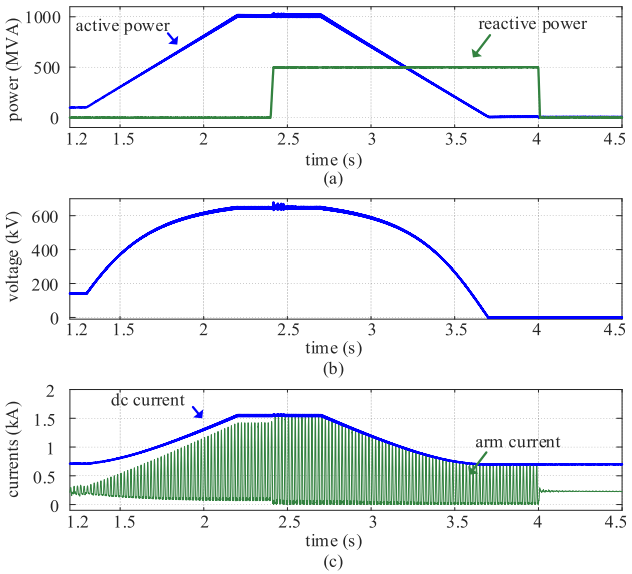

FIGURE 13. Simulation results during power variations: (a) Active and reactive powers; (b) dc voltage; and (c) dc current and arm current.

is similar to that of the conventional HB-MMCs. By the end of the uncontrollable charging, the capacitor voltages are charged to 760V, which is adequately high to supply the controllers.

Then, at 0.7s, the receiving-end UCH-MMC entered the controllable charging. Given the need for dc current to provide the dc bias in the arm currents, a diode is connected with the receiving-end UCH-MMCs in parallel and forms a passage for the dc current. Fig. 12(c) shows that the dc current of the receiving-end UCH-MMC and diode is 470 A (0.3 p.u.) while Fig. 12(d) shows that the capacitor voltages increase until they reach the rated voltage. Then, the dc current reference changes from 0.3 p.u. to the dynamic value calculated by the VVVCM controller. Given that the rated reactive power $Q_N = 500$ Mvar and the active power is 0, the dc current becomes 700 A.

Finally, the sending-end UCH-MMC enters the controllable charging stage at 1.1 s by deblocking the controllers. The output is a small dc voltage that forces the diode to block and the dc current to flow into the sending-end UCH-MMC. The dc current helps to form the unidirectional arm currents of the sending-end UCH-MMC. The capacitor voltage increases until it reaches the rated values.

B. SIMULATION DURING POWER VARIATIONS

Fig. 13 shows the simulation results during power variations. The active power first increases, and then decreases to simulate the variation of dc voltage and current. Fig. 13(b) and (c) respectively show that both the dc voltage and current vary according to the active power. However, even though the

active power reaches 0, the dc current remains to form the unidirectional arm currents. At 2.4 and 4 s, the reactive power steps up and down, respectively. Even if the active power reaches 0, the UCH-MMC can still generate reactive power because of the continuing dc current.

VI. CONCLUSION

The UCH-MMC can reduce the usage of submodule capacitors by utilizing the negative voltage capability of UCH-SMs to increase the modulation index. However, at low active power points, the reactive power capability is limited because the dc current is too low to provide adequate dc bias to form unidirectional arm currents. An approach of retaining a rated dc current even at zero active power has been proposed to enhance the reactive power capability. However, maintaining the rated dc current results in increasing the power losses. This study proposes a new operating mode based on variable dc voltage and current for HVDC systems based on UCH-MMCs. The basic idea of the proposed operating mode is that both the dc current and voltage vary according to the active power, while a lower limit of the dc current is set based on the rated reactive power of the UCH-MMC. Thus, adequate dc bias is provided for the arm current even if the active power reaches 0. In-depth analysis shows that the P–Q capability range is effectively enlarged and the UCH-MMC in the VVVCM retains low capacitor usage. Simulation results verify the analysis.

REFERENCES

[1] A. Lesnicar and R. Marquardt, "An innovative modular multilevel converter topology suitable for a wide power range," in *Proc. IEEE Bologna Power Tech Conf.*, Jun. 2003, p. 6, doi: 10.1109/PTC.2003.1304403.

[2] R. Marquardt, "Modular multilevel converter: An universal concept for HVDC-networks and extended DC-bus-applications," in *Proc. Int. Power Electron. Conf. (ECCE ASIA)*, Jun. 2010, pp. 502–507, doi: 10.1109/IPEC.2010.5544594.

[3] Z. Li, Q. Song, F. An, B. Zhao, Z. Yu, and R. Zeng, "Review on DC transmission systems for integrating large-scale offshore wind farms," *Energy Convers. Econ.*, vol. 2, no. 1, pp. 1–14, Mar. 2021, doi: 10.1049/enc2.12023.

[4] E. Pan, B. Yue, X. Li, Z. Zhao, and Q. Zhu, "Integration technology and practice for long-distance offshore wind power in China," *Energy Convers. Econ.*, vol. 1, no. 1, pp. 4–19, Sep. 2020, doi: 10.1049/enc2.12003.

[5] Q. Song, S. Xu, Y. Zhou, Y. Gim, Z. Li, and Z. Deng, "Active fault-clearing on long-distance overhead lines using a hybrid modular multilevel converter," in *Proc. IEEE 28th Int. Symp. Ind. Electron. (ISIE)*, Jun. 2019, pp. 2033–2038, doi: 10.1109/ISIE.2019.8781312.

[6] V. Hussennether, J. Rittiger, A. Barth, D. Worthington, G. Dell'Anna, M. Rapetti, B. Huhnerbein, and M. Siebert, "Projects BorWin2 and HelWin1—Large scale multilevel voltage-sourced converter technology for bundling of offshore windpower," GIGRE, Paris, France, Tech. Rep. CIGRE B4-306_2012, 2012.

[7] *Dolwin2 Project Sheet*. Accessed: Nov. 5, 2021. [Online]. Available: https://boskalis.com/fileadmin/user_upload/Royal_Boskalis_Westminster_NV/Downloads/Project_sheets/Europe/DolWin2.pdf

[8] C. Zhao, Z. Wang, Z. Li, P. Wang, and Y. Li, "Characteristics analysis of capacitor voltage ripples and dimensioning of full-bridge MMC with zero sequence voltage injection," *IEEE J. Emerg. Sel. Topics Power Electron.*, vol. 7, no. 3, pp. 2106–2115, Sep. 2019, doi: 10.1109/JESTPE.2018.2878411.

[9] C. Zhao, K. Luan, H. Zhang, Z. Li, P. Wang, and Y. Li, "Enhancement of ZSVI by circulating current injection for full-bridge MMC with low energy storage requirements," *IEEE J. Emerg. Sel. Topics Power Electron.*, vol. 8, no. 4, pp. 4075–4085, Dec. 2020, doi: 10.1109/JESTPE.2019.2927690.

[10] L. Baruschka and A. Mertens, "Comparison of cascaded H-bridge and modular multilevel converters for BESS application," in *Proc. IEEE Energy Convers. Congr. Expo.*, Sep. 2011, pp. 909–916, doi: 10.1109/ECCE.2011.6063868.

[11] K. Ilves, S. Norrga, and H.-P. Nee, "On energy variations in modular multilevel converters with full-bridge submodules for AC-DC and AC-AC applications," in *Proc. 15th Eur. Conf. Power Electron. Appl. (EPE)*, Sep. 2013, pp. 1–10, doi: 10.1109/EPE.2013.6634324.

[12] W. Lin, D. Jovcic, S. Nguefeu, and H. Saad, "Full-bridge MMC converter optimal design to HVDC operational requirements," *IEEE Trans. Power Del.*, vol. 31, no. 3, pp. 1342–1350, Jun. 2016, doi: 10.1109/TPWRD.2015.2475130.

[13] Y. Lyu, C. Li, Y.-H. Hsieh, F. C. Lee, Q. Li, and R. Xu, "Capacitor voltage ripple reduction with state trajectory analysis for modular multilevel converter," in *Proc. IEEE Appl. Power Electron. Conf. Expo. (APEC)*, Mar. 2017, pp. 1829–1836, doi: 10.1109/APEC.2017.7930947.

[14] J. Hu, M. Xiang, L. Lin, M. Lu, J. Zhu, and Z. He, "Improved design and control of FBSM MMC with boosted AC voltage and reduced DC capacitance," *IEEE Trans. Ind. Electron.*, vol. 65, no. 3, pp. 1919–1930, Mar. 2018, doi: 10.1109/TIE.2017.2739679.

[15] C. Zhao, Y. Li, Z. Li, P. Wang, X. Ma, and Y. Luo, "Optimized design of full-bridge modular multilevel converter with low energy storage requirements for HVDC transmission system," *IEEE Trans. Power Electron.*, vol. 33, no. 1, pp. 97–109, Jan. 2018, doi: 10.1109/TPEL.2017.2660532.

[16] Q. Song, W. Yang, B. Zhao, S. Xu, H. Rao, and Z. Zhu, "Energy storage requirement reduction using negative-voltage states of a full-bridge modular multilevel converter," *IEEE Trans. Power Electron.*, vol. 34, no. 6, pp. 5243–5255, Sep. 2019, doi: 10.1109/TPEL.2018.2869464.

[17] W. Yang, Q. Song, S. Xu, H. Rao, and W. Liu, "An MMC topology based on unidirectional current H-bridge submodule with active circulating current injection," *IEEE Trans. Power Electron.*, vol. 33, no. 5, pp. 3870–3883, May 2018, doi: 10.1109/TPEL.2017.2722011.

[18] G. J. M. de Sousa and M. L. Heldwein, "Modular multilevel converter based unidirectional medium/high voltage drive system," in *Proc. 39th Annu. Conf. IEEE Ind. Electron. Soc. (IECON)*, Nov. 2013, pp. 1037–1042, doi: 10.1109/IECON.2013.6699276.

[19] W. Yang, Q. Song, and B. Zhao, "Energy storage requirement and low capacitance operation of unidirectional current H-bridge modular multilevel converters," *IEEE Trans. Power Electron.*, vol. 34, no. 12, pp. 11748–11759, Dec. 2019, doi: 10.1109/TPEL.2019.2910456.

[20] X. Yu, Y. Wei, and Q. Jiang, "New submodule circuits for modular multilevel current source converters with DC fault ride through capability," in *Proc. IEEE Appl. Power Electron. Conf. Expo. (APEC)*, Mar. 2016, pp. 1468–1474, doi: 10.1109/APEC.2016.7468062.

[21] A. Lesnicar, "Neuartiger modularer mehrpunktumrichter M2C für netzkupplungsanwendungen," Ph.D. thesis, Univ. Bundeswehr München, München, Germany, 2008.

[22] K. Ilves, S. Norrga, L. Harnefors, and H.-P. Nee, "On energy storage requirements in modular multilevel converters," *IEEE Trans. Power Electron.*, vol. 29, no. 1, pp. 77–88, Jan. 2014, doi: 10.1109/TPEL.2013.2254129.

[23] W. Yang, Q. Song, and W. Liu, "Decoupled control of modular multilevel converter based on intermediate controllable voltages," *IEEE Trans. Ind. Electron.*, vol. 63, no. 8, pp. 4695–4706, Aug. 2016, doi: 10.1109/TIE.2016.2549001.

ZHENGXUAN LI (Graduate Student Member, IEEE) was born in Beijing, China, in 1995. He received the B.S. degree from North China Electric Power University, Beijing, in 2018. He is currently pursuing the Ph.D. degree with Tsinghua University, Beijing.

His current research interests include modular multilevel converter, wind power, and VSC-HVDC transmission systems.

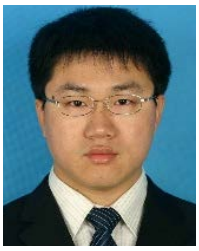

LINLIN WU (Associate Member, IEEE) was born in Hebei, China, in 1986. He received the M.S. degree from Tsinghua University, Beijing, China, in 2010.

He is currently working at State Grid Jibei Electric Power Company Ltd., Research Institute (North China Electric Power Research Institute Company Ltd.), Beijing. His current research interests include renewable energy grid-connected control technologies and characteristics of VSC-HVDC transmission systems.

QIANG SONG (Senior Member, IEEE) was born in Changchun, China, in 1975. He received the B.E.E. and Ph.D. degrees in electrical engineering from Tsinghua University, Beijing, China, in 1998 and 2003, respectively.

From 2003 to 2008, he was a Lecturer with the Department of Electrical Engineering, Tsinghua University. Since 2008, he has been an Associate Professor with the Department of Electrical Engineering, Tsinghua University. His main research interests include high-power electronic interfaces for utility systems, flexible ac transmission systems, VSC-HVDC systems, and custom power quality.

XIAOYANG DENG was born in Hebei, China, in 1989. He received the Ph.D. degree from Beijing Jiaotong University, Beijing, China, in 2018.

He is currently working at State Grid Jibei Electric Power Company Ltd., Research Institute (North China Electric Power Research Institute Company Ltd.), Beijing. His current research interests include characteristics of renewable energy and multi-terminal flexible DC transmission systems.

BIAO ZHAO (Senior Member, IEEE) was born in Hubei, China, in 1987. He received the B.S. degree from the Department of Electrical Engineering, Dalian University of Technology, Dalian, China, in 2009, and the Ph.D. degree from the Department of Electrical Engineering, Tsinghua University, Beijing, China, in 2014.

He is currently an Associate Professor with the Department of Electrical Engineering, Tsinghua University. His research interests include high-power converters, high-power semiconductor devices, and flexible dc transmission and distribution systems. He is a Senior Member of the Chinese Society for Electrical Engineering and the Chinese Electro-Technical Society.

YUNHONG LI was born in Jilin, China, in 1988. She received the M.S. degree from Tsinghua University, Beijing, China, in 2013.

She is currently working at State Grid Jibei Electric Power Company Ltd., Research Institute (North China Electric Power Research Institute Company Ltd.), Beijing. Her current research interests include VSC-HVDC transmission systems, sub/super-synchronic oscillation, and voltage stability of wind power systems.

KAILUN WANG was born in Henan, China, in 1998. He received the B.E. degree in electrical engineering from Tsinghua University, Beijing, China, in 2020, where he is currently pursuing the Ph.D. degree with the Department of Electrical Engineering.

His research interests include modular multilevel converter and VSC-HVDC transmission systems.